

The fine-structure parameters and Zeeman splitting of levels of the configurations $1sni$ ($n = 7 - 10$) of the helium atom

Galina Pavlovna Anisimova¹, Igor Cheslavovich Mashek¹, Olga Aleksandrovna Dolmatova¹, Anna Petrovna Gorbenko^{1,*}, Robert Ivanovich Semenov¹, Martin Luther Tchoffo², Galina Aleksandrovna Tsygankova¹

¹Saint-Petersburg State University, Saint-Petersburg, Russian Federation

²University of Dschang, Po Dschang, Cameroon

Email address:

spbgor@mail.ru (A.P. Gorbenko), mtchoffo2000@yahoo.fr (M. Tchoffo), olgadolmatova@gmail.com (O.A. Dolmatova)

To cite this article:

Galina Pavlovna Anisimova, Igor Cheslavovich Mashek, Olga Aleksandrovna Dolmatova, Anna Petrovna Gorbenko, Robert Ivanovich Semenov, Martin Luther Tchoffo, Galina Aleksandrovna Tsygankova, The Fine-Structure Parameters and Zeeman Splitting of Levels of the Configurations $1sni$ ($n = 7 - 10$) of the Helium Atom. *American Journal of Modern Physics*. Vol. 3, No. 4, 2014, pp. 143-151. doi: 10.11648/j.ajmp.20140304.11

Abstract: By the semiempirical method in the intermediate coupling, the fine-structure parameters of $1sni$ Helium atom configurations were determined from the resolution of the system of nonlinear equations by the Newton's iteration method. The system is based on an energy operator nondiagonal matrix, in which the following interactions were taken into account: the electrostatic, the spin-orbit (own and other) and the spin-spin interactions. With the obtained fine-structure parameters, the numerical diagonalization of the energy operator matrix was effected. The result was the calculated energies, coinciding to last digit with the experimental analogues, and the intermediate coupling coefficients. The gyromagnetic ratios of the 3I_6 and 1I_6 levels were determined and the appreciation of the character of the coupling in the consider systems was done. The Zeeman structure of the $1sni$ configurations was investigated. Its particularity and the domain of linearity of the magnetic field were determined. The gyromagnetic ratios of all the four configurations levels were calculated by the magnetic component splitting.

Keywords: Energy Operator Matrix, LSJM Representation, Uncoupled Moments Representation, Zeeman Splitting, Magnetic Field, Crossing and Anticrossings of the Magnetic Sublevels

1. Introduction

The highly excited $1sni$ configurations of the Helium atom are virtually not investigated. Only experimental energy levels of fine structure are available [1, 2]. This is why it is possible to calculate the fine-structure parameters by the semi-empirical method. With their help (by diagonalizing the energy matrix operator), one can determine the coupling coefficients and the gyromagnetic ratios which are very important characteristics of atomic systems. Furthermore one can prognosticate the Zeeman splitting particularity (the crossings and anticrossings of magnetic sublevels), and also determine the g-factors of the configuration levels in linear domain of the magnetic field.

2. The Energy Spectrum of $1sni$ Helium Configurations and the Transformation Coefficients of LS-coupling Wave Functions

The $1sni$ Helium atom configurations are 4-level systems totally isolated from all other configurations. As an example in the Fig.1 it is shown the energy spectrum of the lowest $1s7i$ configuration. For the rest of the configurations with $n \geq 8$ the intervals between levels are given in inverse centimeters.

	$1s8i$	$1s9i$	$1s10i$
$\Delta E (^3I_7-^3I_6)$	0.00031	0.00022	0.00016
$\Delta E (^3I_5-^3I_7)$	0.00028	0.00020	0.00014
$\Delta E (^1I_6-^3I_5)$	0.00022	0.00016	0.00011

It is seen that the considered system deviates a lot from the LS-coupling, which is characterized by nearly scattered triplet levels and considerably far from their singlet level ($1snp$ and $1snd$ configurations). The energy spectrums of all highly excited $1snl$ with $l \geq 3$ ($1snf$, $1sng$ and so on) configurations are quartet levels with approximately the same distance between them.

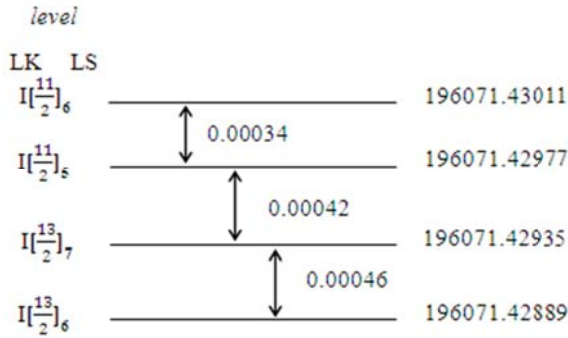


Figure 1. Energy spectrum of the $1s7i$ configuration of the helium atom. On the left – the notation of levels in LK- and LS- coupling.

In order to appreciate the coupling character of the considered system in relation to other types of vector couplings, it is necessary to calculate the g-factors in all types of coupling and compare them with similar values in the intermediate (real) coupling. To this effect one has to obtain first the transformation coefficients of wave functions of one type of coupling through the wave functions of the other type of coupling. The corresponding formulae have the following form [3]:

$$\begin{aligned}
 & LS \overset{\rightarrow}{\leftarrow} LK \\
 & [l_1 l_2(L), s_1 s_2(S), J] | l_1 l_2(L) s_1(K) s_2(J) \rangle = \\
 & = (-1)^{s_1+s_2+L+J} \delta(L, L') \delta(l_1 l_2 L) \times \\
 & \times [(2S+1)(2K+1)]^{\frac{1}{2}} \begin{Bmatrix} L & s_1 & K \\ s_2 & J & S \end{Bmatrix} \quad (2)
 \end{aligned}$$

Here $K = L + s_1$, $J = K + s_2$

$$\begin{aligned}
 & LS \overset{\rightarrow}{\leftarrow} jK \\
 & [l_1 l_2(L), s_1 s_2(S), J] | l_1 s_1(j_1) l_2(K) s_2(J) \rangle = \\
 & = (-1)^{l_2-s_2+j_1-J} [(2L+1)(2S+1)(2j_1+1)]^{\frac{1}{2}} \times \\
 & \times (2K+1)^{\frac{1}{2}} \begin{Bmatrix} l_1 & l_2 & L \\ K & s_1 & j_1 \end{Bmatrix} \begin{Bmatrix} s_1 & s_2 & S \\ J & L & K \end{Bmatrix} \quad (3)
 \end{aligned}$$

Here $K = j_1 + l_2$ ($j_1 = l_1 + s_1$); $J = K + s_2$. The expressions in the brackets of formulae (2) and (3) are Wigner 6j-symbols.

They are calculated using the monograph formulae [4], just like 9j-symbols in (4) (see below).

$$\begin{aligned}
 & LS \overset{\rightarrow}{\leftarrow} jj \\
 & [l_1 l_2(L), s_1 s_2(S), J] | l_1 s_1(j_1), l_2 s_2(j_2), J \rangle = \\
 & = [(2L+1)(2S+1)(2j_1+1)]^{\frac{1}{2}} \times \\
 & \times (2j_2+1)^{\frac{1}{2}} \begin{Bmatrix} l_1 & s_1 & j_1 \\ l_2 & s_2 & j_2 \\ L & S & J \end{Bmatrix} \quad (4)
 \end{aligned}$$

Here $j_1 = l_1 + s_1$; $j_2 = l_2 + s_2$; $J = j_1 + j_2$. For $nsn'i$ configuration: $l_1 = 0$, $l_2 = 6$, $L = 6$. The results of calculation with respect to formulae (2)-(4) are presented in the Table 1.

Table 1. Transformation coefficients of wave functions of one type of coupling through the wave functions of the other type of coupling and the corresponding gyromagnetic ratios of $nsn'i$ configurations

$LS \overset{\rightarrow}{\leftarrow} LK$			
LKJ	3I_6	1I_6	g^{LK}
$I[\frac{11}{2}]_6$	$\sqrt{\frac{7}{13}}$	$-\sqrt{\frac{6}{13}}$	$\frac{1}{78}(77g_l + g_s) = 1.012850$
$I[\frac{13}{2}]_6$	$\sqrt{\frac{6}{13}}$	$\sqrt{\frac{7}{13}}$	$\frac{1}{91}(90g_l + g_s) = 1.011015$

$LS \overset{\rightarrow}{\leftarrow} jK$			
$j_1 K J$	3I_6	1I_6	g^{jK}
$\frac{1}{2} [\frac{11}{2}]_6$	$-\sqrt{\frac{7}{13}}$	$\sqrt{\frac{6}{13}}$	$\frac{1}{78}(77g_l + g_s)$
$\frac{1}{2} [\frac{13}{2}]_6$	$\sqrt{\frac{6}{13}}$	$\sqrt{\frac{7}{13}}$	$\frac{1}{91}(90g_l + g_s)$

$LS \overset{\rightarrow}{\leftarrow} jj$			
$j_1 K J$	3I_6	1I_6	g^{jj}
$[\frac{1}{2} \frac{11}{2}]_6$	$\sqrt{\frac{7}{13}}$	$\sqrt{\frac{6}{13}}$	$\frac{1}{78}(77g_l + g_s)$
$[\frac{1}{2} \frac{13}{2}]_6$	$-\sqrt{\frac{6}{13}}$	$\sqrt{\frac{7}{13}}$	$\frac{1}{91}(90g_l + g_s)$

$$^3I_7: g^{LS} = \frac{1}{7}(6g_l + g_s) = 1.143189;$$

$$^3I_6: g^{LS} = \frac{1}{42}(41g_l + g_s) = 1.023865;$$

$$^3I_5: g^{LS} = \frac{1}{6}(7g_l - g_s) = 0.832947;$$

$$^1I_6: g^{LS} = g_l = 1.0$$

Remark: g_l and g_s are the orbital and the spin gyromagnetic ratios. They are given as: $g_l = 1.0$; $g_s = 2.00232$.

It is seen that for LK, jK, jj types of vector coupling the coefficients of the transformation have the same value, but have different signs. The normalization and orthogonality conditions are fulfilled. In the last column in the Table 1 the gyromagnetic ratios of two levels with the same value of $J = 6$ in different type of vector couplings are given. They are

calculated by this formula:

$$g = \alpha_{ik}^2 g_k^{LS} \quad (5)$$

Here α_{ik} are transformation coefficients from the Table 1 (i is the row number, k the column number); g^{LS} are the LS-coupling gyromagnetic ratios, calculated [5,6] with respect to formula:

$$g^{LS} = \frac{J(J+1)+L(L+1)-S(S+1)}{2J(J+1)} g_l + \frac{J(J+1)+S(S+1)-L(L+1)}{2J(J+1)} g_s \quad (6)$$

Their analytical expressions and their numerical values are given at the end of the Table 1.

As the transformation coefficients from the Table 1 are squared (5), their signs are not important in the transition from one representation to the other. This is why the gyromagnetic ratios of the levels 3I_6 and 1I_6 are the same in LK , jK , jj coupling types. The two other levels 3I_7 and 3I_5 are unique in the configuration with indicated values of J ; their g -factors are supposed to be independent of the type of coupling and are equal to the corresponding LS-coupling analogue. Below, we will see (by during the calculation of the g -factors with using the Zeeman splitting levels), how this is verified in the real situations (the intermediate coupling).

3. Energy Operator Matrix and the Method of Calculation of Fine-Structure Parameters

The energy operator matrix is the basis of the numerical calculation of the fine-structure parameters. Independent results are presented in [7] for calculations with respect to the spin-other orbit, the spin-spin and the orbit-orbit interactions. Let's bring the complete energy operator matrix of $nsin'$ configurations in the form in which it is used for the numerical calculation of the fine-structure parameters by semi-empirical methods:

$$\begin{aligned} {}^3I_6 {}^3I_6 &= F_0 - G_6 - \frac{1}{2}\xi_2 + S_2 + \frac{6}{13}S_4 = C_1; \\ {}^3I_7 {}^3I_7 &= F_0 - G_6 + 3\xi_2 - \frac{86}{5}S_2 - \frac{36}{13}S_4 = C_2; \\ {}^3I_5 {}^3I_5 &= F_0 - G_6 - \frac{7}{2}\xi_2 + \frac{245}{11}S_2 + \frac{42}{13}S_4 = C_3; \\ {}^1I_6 {}^1I_6 &= F_0 + G_6 = C_4; \\ {}^3I_6 {}^1I_6 &= -\frac{\sqrt{42}}{2}\xi_2 - \sqrt{42}S_2^* = C_5 \end{aligned} \quad (7)$$

Here F_0 and G_6 are the direct and the exchange Slater radial integrals respectively (the angular coefficient 1/13

for radial integral G_6 in expressions (7) are omitted in order to reduce writing); ξ_2 is the radial integral of the spin-other orbit interaction of the i -electron; S_2 is the direct radial Marvin integral [7], united by the spin-spin and the spin-other orbit interactions (the sign «*» in the matrix element C_5 means that S_2 belongs only to spin-other orbit interaction); S_4 is the exchange radial integral K_k [3], corresponding to spin-other orbit interaction and related to Marvin integral. Let's note that in the present paper the exchange part of energy operator of spin-other orbit interaction is described by the radial integral K_k , which is related to the radial integral K'_k in [7] in the following manner [3]:

$$K_k = -2k(k+1)K'_k \quad (8)$$

The parameter of summation k in (8) takes the values [3]:

$$k = |l_1 - l_2|, |l_1 - l_2| + 2, \dots, l_1 + l_2, \quad (9)$$

That means for si configuration: $k = 6$, so $K_k = -84K'_k$. This was taken into account in the angular coefficient in S_4 integral (our notation for the radial integral K_k).

The radial integrals in (7) are the unknown fine-structure parameters. From (7), it is seen that the fine-structure parameters are 5 and the 4 levels in the configuration. For this reason, the following set of equations was used in the numerical determination of the fine structure:

$$\begin{aligned} 1) \quad C_2 - \varepsilon_2 &= 0; \\ 2) \quad C_3 - \varepsilon_3 &= 0; \\ 3) \quad C_1 + C_4 - (\varepsilon_1 + \varepsilon_4) &= 0; \\ 4) \quad C_1 C_4 - C_5^2 - \varepsilon_1 \varepsilon_4 &= 0; \\ 5) \quad \alpha_{11}(C_1 - \varepsilon_1) + \alpha_{12} C_5 &= 0; \\ 6) \quad \alpha_{11} C_5 - \alpha_{12}(C_1 - \varepsilon_4) &= 0; \\ 7) \quad \alpha_{11}^2 + \alpha_{12}^2 &= 1 \end{aligned} \quad (10)$$

Here ε_i are the fine structure experimental energy levels increase in number with respect to [2]. C_i is the energy operator matrix (7), divided by $J - 2$ matrices of first rank ($J = 7, J = 5$, equations 1) and 2)) and one matrix of second rank with $J = 6$ (equation 3) and 4)). Equations 5) and 6) are the result of the unitary transformation of the nondiagonal Hermitian second rank matrix to the diagonal form:

$$|\varepsilon_i| = \alpha_{ik} |C_i| \alpha_{ki} \quad (11)$$

Some additional unknowns appear in these equations; the unitary transformation coefficients α_{11} and α_{12} (the condition of their orthogonality was taken into account in equations 5) and 6)). The last equation in the system (10) is the normalization condition of coupling coefficients.

The system of equations (3 linear and 4 quadratic) for 7 unknown values (5 parameters and 2 coupling coefficients)

was solve by Newton's iteration method, which required the zero approximation. The first zero approximations were obtained from the resolution of the linear system of equations (the matrix spur, or the Slater's rule of diagonal sums) for the basis parameters F_0 , G_6 , ξ_2 . The rest of parameters were supposed to be equal to zero. Further with these numerical values of the parameters, the diagonalization of the second rank matrix was done, from where the calculated energies (eigen values) and coupling coefficients (eigen vectors) were obtained. Knowing the latter from (11) one determines the numerical values of the elements of second rank no diagonal matrices C_1 , C_4 , C_5 . The numerical values of elements of the first rank matrix were added to them. We obtained 5 linear equations for 5 fine-structure parameters as the approximations to the resolution of the system of equations (10). At each step of the calculations, the numerical diagonalization of the corresponding energy operator matrices was done and the cycle repeated until the different between the calculated and the experimental energies decreased practically to zero. This permits further to study the Zeeman structure and its particularity.

4. Results of the Numerical Calculation and Discussion

The fine-structure parameters of helium $1sni$ ($n = 7 - 10$) configurations are presented in the Table 2. During the calculation, the relative energies (intervals energies) rather than the absolute energies were used. The ground state energy of 3I_6 was set equal to zero. The absolute energy levels of 3I_6 , which are added to the values of the parameter F_0 , shown in the table for the determination of the absolute energies of the rest of the level configurations, are given at the end of the Table 2. The using of relative energies is more convenient as compared to the absolute values because higher orders are excluded and the difficulty in the solution of the system of equations (10) is considerably reduced. All the solutions were obtained when the difference between the calculated and the experimental energies was $(10^{-10} - 10^{-13}) \text{ cm}^{-1}$.

Table 2. The fine-structure parameters ($T^*10^5 \text{ cm}^{-1}$) of the configurations $1sni$ ($n = 7 - 10$) of the helium atom

Parameters	1s7i	1s8i	1s9i	1s10i
F_0	69.02421	46.24070	32.47615	23.67514
G_6	13.38073	8.96385	6.29540	4.58928
ζ_i	-36.91836	-24.73223	-17.37000	-12.66271
S_2	9.69720	6.49626	4.56240	3.32597
S_4	-96.78650	-64.83851	-45.53705	-33.19637

Note: Absolute energies of the low levels in inverse centimeters [2]: 196071.428891148 (1s7i), 196596.251052062 (1s8i), 196956.067465189 (1s9i), 197213.442016 (1s10i)

From the Table 2 it's seen that, with increasing principal quantum number n of i -electron the variation of all fine-structure parameters is harmonic, which indirectly testifies their viability. The constant ξ_2 (ξ_i) is negative, as it must be for the reverse triplet. It is also seen that, in the considered configurations the role of magnetic interactions (parameters ξ_2 , S_2 , S_4) increases as compared to electrostatic interactions. This is explained by the fact that there is recess from the LS-coupling (see Fig.1 and (1)). As it is significant, one shows the intermediate coupling coefficients and the gyromagnetic ratios. They are presented in the Table 3 (g) together with their vector analogs (g^{LS} and g^{LK}). In the Table 4 the tendency of their variation with respect to all the rest of the lower $1sni$ ($l = 1 - 5$) Helium configurations is observed.

Table 3. Expansion coefficients of wave functions in terms of the LS-coupling scheme and the gyromagnetic ratios of the $1sni$ Helium configurations.

Configur- ation	3I_6 (α_{11})	1I_6 (α_{12})	g (3I_6)	g (1I_6)
1s7i	0.8234315962	-0.56741555	1.0161813	1.0076835
1s8i	0.8234294703	-0.567418635	1.0161812	1.0076836
1s9i	0.8234261112	-0.5674235097	1.0161810	1.0076837
1s10i	0.8234246509	-0.5674256288	1.01618098	1.0076838

$$g^{LS}(^3I_6) = 1.023685, \quad g^{LK}(|\frac{13}{2}\rangle_6) = 1.011015,$$

$$g^{LS}(^1I_6) = 1.0, \quad g^{LK}(|\frac{11}{2}\rangle_6) = 1.012850$$

Table 4. Comparison of the intermediate coupling coefficients and the gyromagnetic ratios in the lower $1sni$ ($l = 1 - 5$) Helium atom configurations

	α_{11}	α_{12}	g (3L_j)	g (3L_j)
1s2p	0.99999997	$-2.451 \cdot 10^{-4}$	1.50115997 (3P_1)	1.00000003 (1P_1)
1s3d	0.9999769	$-6.798 \cdot 10^{-3}$	1.1670456 (3D_2)	1.00000772 (1D_2)
1s4f	0.879548	-0.475810	1.064617 (3F_3)	1.018910 (1F_3)
1s5g	0.859054	-0.511886	1.036984 (3G_4)	1.013132 (1G_4)
1s6h	0.839430	-0.543468	1.023543 (3H_5)	1.009868 (1H_5)

$$g^{LS}(^3P_1) = 1.501116; \quad g^{LS}(^3D_2) = 1.1670533; \quad g^{LS}(^3F_3) = 1.0835266;$$

$$g^{LS}(^3G_4) = 1.050116; \quad g^{LS}(^3H_5) = 1.0334106; \quad g^{LS}(^1L_j) = g_l = 1.0$$

Note. The results of the table are our semi-empirical calculation (the precised non-earlier published data).

From the Table 4, it's seen that for the $1s2p$ configuration, the coupling coefficients on the main diagonal are near unity. That is why the numerical values of the g -factors in the intermediate coupling coincide practically with the LS-coupling values (presented at the end of the Table 4). For the $1s3d$ configuration the coupling coefficients on the main diagonal are less as compared to the $1s2p$ configuration, but also near unity, and the corresponding g -factors coincides practically with analogous LS-coupling. This testifies that the $1snp$ and the $1sni$ configurations are near the LS-coupling. Starting from $1snf$ configurations,

the coupling coefficients on the main diagonal are considerably different from unity, the gyromagnetic relations also show the regress from the LS-coupling. With increasing second electron orbital momentum l_2 , the coupling coefficients on the main diagonal decrease, that means regress from the LS-coupling. The situation is similar for the considered upper $1sni$ configuration (see the Table 3).

From the Table 3 it follows that, with increasing quantum number n of i -electron the coupling coefficients and the gyromagnetic ratios remain stable. The comparison of the g -factors calculated in the intermediate coupling with their vector analogs (g^{LS} and g^{LK}) show, that in the considered systems, the intermediate coupling between the LS and LK- types of vector coupling is realized, near to LK-coupling. That is why the spectral energies (see Fig.1 and (1)) are presented as quartet levels with approximately the same distance between them. This can be explained by the fact that, in the $1snp$ and $1snd$ configurations the disposition of the levels in the reverse triplet is correct, namely $^3L_{J+1}$ (the lower), 3L_J (the middle), $^3L_{J-1}$ (the upper level of the triplet). The singlet level 1L_J is considerably far from the triplet system. Here the 3L_J and 1L_J levels interact. They are responsible for the intermediate coupling (see up the second rank energy operator non diagonal matrix (7)). Furthermore the 3L_J level is at the middle of the triplet, while in the $1snl$ ($l \geq 3$) configurations the correct disposition of the triplet levels is violated, the lower level becomes 3L_J , the middle - $^3L_{J+1}$, the upper $^3L_{J-1}$. The singlet level 1L_J approaches the triplet. Not only does the triplet middle level interact with the singlet upper level, but also does the triplet system lower level interact with the singlet upper level.

5. Zeeman Splitting of the Levels

It is known, that in the magnetic field, the degeneracy in the magnetic quantum number M is removed [5,6] and the energy operator matrix is separated into matrices related to M . In the considered configurations, $M = \pm 7$ (for the first rank), $M = \pm 6$ (for the third rank), all the rest of the matrices with $M = \pm 5, \pm 4, \pm 3, \pm 2, \pm 1$ and 0 are of rank four. Let's write in the general form, the energy operator fourth rank matrix taking in to account the atom's interaction with the magnetic field (the corresponding elements are denoted by *). It has the form:

$$\begin{matrix}
 & ^3I_6 & ^3I_7 & ^3I_5 & ^1I_5 \\
 ^3\tilde{I}_6 & C_1 + * & * & * & C_5 \\
 ^3\tilde{I}_7 & * & C_2 + * & 0 & 0 \\
 ^3\tilde{I}_5 & * & 0 & C_3 + * & 0 \\
 ^1\tilde{I}_5 & C_5 & 0 & 0 & C_4 + *
 \end{matrix} \quad (12)$$

The third rank matrix ($M = \pm 6$) is obtained by deleting the third row and the third column in (12). The first rank

matrix has one element $^3\tilde{I}_7^3I_7 = C_2 + *$.

The energy operator of atom interaction with the magnetic field has the form [5,6]:

$$W = \mu_0 g J H \quad (13)$$

The role of radial integral in (13) is played by the Bohr magneton $\mu_0 = 4.6686437 * 10^{-5} (\frac{cm^{-1}}{oe})$ [8].

The operator matrix elements in (13) are calculated with the use of formulae (see also [6]):

$$\begin{aligned}
 |W_{ii}| = & \left[\frac{J(J+1) + L(L+1) - S(S+1)}{2J(J+1)} g_l + \right. \\
 & \left. + \frac{J(J+1) + S(S+1) - L(L+1)}{2J(J+1)} g_s \right] \times \\
 & \times \mu_0 H M \quad (14)
 \end{aligned}$$

They are different from zero in the conditions: $\Delta J = \Delta S = \Delta L = 0$. The expression in the brackets in (14) is the gyromagnetic ratio divided into the orbital and spin parts. The values g_l and g_s in most of the literature are different. In this paper the values used are: $g_l = 1.0$, $g_s = 2.00232$.

The nondiagonal matrix elements have the form:

$$\begin{aligned}
 |W_{ij}| = & \sqrt{\frac{(J-L+S+1)(J+L-S+1)(J+L+S+2)(L+S-J)}{4(J+1)^2(2J+1)(2J+3)}} \times \\
 & \times [(J+1)^2 - M^2]^{\frac{1}{2}} \times (g_l - g_s) \mu_0 H \quad (15)
 \end{aligned}$$

$|W_{ij}| \neq 0$ in the conditions $\Delta J = \pm 1$, $\Delta S = \Delta L = 0$; $J = J_{min}$.

We obtained formulae (14) and (15) earlier with wave functions of the uncoupled moments representation with further transfer to the LSJM representation for the $npn'p$ configurations. They are true for all the rest of the two-electron configurations. The results of calculation through formulae (4) and (15) are presented in the Table 5. If in expressions (14) and (15) one puts $g_l = 1$, $g_s = 2$, as it was done in [6], then our results coincide completely with the matrix elements in [6] with some reserves: in the nondiagonal matrix elements in [6], there appears a factor $(g_l - g_s)$, that means the square root is taken with the minus sign (in [6] the sign of the square root is not indicated).

Let's note that, in the LSJM representation (LS-coupling approximation) the energy operator matrix (12) is more compact as compared to matrices in the uncoupled moments representation, since in it one uses the same "basis" elements C_i for any value of the quantum magnetic number M . The dependence of M (the * elements in formula (12)) is determined according to formulae (14) and (15), see the Table 5.

Table 5. Energy operator matrix elements for atom interaction with the magnetic field

Matrix element	M = ±7	M = ±6	M = ±5	M = ±4	M = ±3	M = ±2	M = ±1	M = 0
$^3I_7^3I_7$	$\pm(6g_l + g_s)$	$\pm\frac{6}{7}(6g_l + g_s)$	$\pm\frac{5}{7}(6g_l + g_s)$	$\pm\frac{4}{7}(6g_l + g_s)$	$\pm\frac{3}{7}(6g_l + g_s)$	$\pm\frac{2}{7}(6g_l + g_s)$	$\pm\frac{1}{7}(6g_l + g_s)$	0
$^3I_6^3I_6$		$\pm\frac{1}{7}(41g_l + g_s)$	$\pm\frac{5}{42}(41g_l + g_s)$	$\pm\frac{2}{21}(41g_l + g_s)$	$\pm\frac{1}{14}(41g_l + g_s)$	$\pm\frac{1}{21}(41g_l + g_s)$	$\pm\frac{1}{42}(41g_l + g_s)$	0
$^3I_5^3I_5$			$\pm\frac{5}{6}(7g_l - g_s)$	$\pm\frac{2}{3}(7g_l - g_s)$	$\pm\frac{1}{2}(7g_l - g_s)$	$\pm\frac{1}{3}(7g_l - g_s)$	$\pm\frac{1}{6}(7g_l - g_s)$	0
$^1I_6^1I_6$		$\pm 6g_l$	$\pm 5g_l$	$\pm 4g_l$	$\pm 3g_l$	$\pm 2g_l$	$\pm g_l$	0
$^3I_7^3I_6$		$\frac{\sqrt{6}}{7}(g_l - g_s)$	$\frac{12}{7\sqrt{13}}(g_l - g_s)$	$\frac{3\sqrt{22}}{7\sqrt{13}}(g_l - g_s)$	$\frac{4\sqrt{15}}{7\sqrt{13}}(g_l - g_s)$	$\frac{3\sqrt{30}}{7\sqrt{13}}(g_l - g_s)$	$\frac{12\sqrt{2}}{7\sqrt{13}}(g_l - g_s)$	$\frac{\sqrt{6}}{\sqrt{13}}(g_l - g_s)$
$^3I_6^3I_5$			$\frac{\sqrt{77}}{6\sqrt{13}}(g_l - g_s)$	$\frac{\sqrt{35}}{3\sqrt{13}}(g_l - g_s)$	$\frac{\sqrt{21}}{2\sqrt{13}}(g_l - g_s)$	$\frac{2\sqrt{14}}{3\sqrt{13}}(g_l - g_s)$	$\frac{7\sqrt{5}}{6\sqrt{13}}(g_l - g_s)$	$\frac{\sqrt{7}}{\sqrt{13}}(g_l - g_s)$

} $\times \mu_0 H$

Zero energy residuals (the obtained in this work energy levels are almost coincide with corresponding experimental quantities [2]) permits the investigation the Zeeman splitting and its particularity – the crossings and the anticrossings of magnetic components as a prognostic for the future experiments in this domain. Furthermore, it is interesting to determine with the help of the Zeeman splitting the g-factors for all four levels of the considered configurations and appreciate the character of the coupling in them.

Gyromagnetic ratios can be calculated from Zeeman splittings only in a linear range, in which the spacings between positive and negative values of M and M = 0 are the same. The linear range is established as follows: At certain points of the magnetic field, the numerical diagonalization of energy operator matrices (12) is provided for the values of the quantum magnetic number M = +1, 0, -1. In this condition the distance (ΔE) between the magnetic components with positive and negative values of M with respect to the component with M = 0 must be the same. As an example, for the $1s7i$ configuration, the Table 6 shows results of the diagonalization of the energy operator matrix (12) for the values M = +1, 0, -1 when H = 0.05 Oe (the linear range is presented in the Table 7). For comparison in the Table 6 the same results for H = 0 are presented (the upper part of the table). It is seen that, when H = 0 the energy levels of the fine structure (the first column) coincide with the experimental equivalents [2]. Expansion the coefficients of wave function in terms of the LS-coupling scheme on the main diagonal are equal to unity precisely for 3I_7 and 3I_5 levels. This shows the independence of these levels of the type of coupling, and the corresponding g-factors are equal to their LS-coupling analogues (see the lower part of the Table 1). The 3I_6 and 1I_6 levels with the same value of J = 6 have exactly the same coupling coefficients on the main diagonal with the corresponding gyromagnetic ratios as in the Table 3.

From the Table 6 it is also seen that when the magnetic field is switched on (M = +1, 0, -1), the coupling coefficients on the main diagonal for the 3I_7 and 3I_5 levels are close to, but not equal to unity. In the corresponding rows the nondiagonal elements (near zero) appear, and the matrix of coefficients is no more quasi-diagonal, as in the case of H =

0. Comparing the difference of energies of Zeeman components ΔE (M = +1, 0) and ΔE (M = -1, 0) for all the four configuration levels, we see that they are the same. All what is said is true for all the rest of the considered $1s8i$, $1s9i$, $1s10i$ configurations. For them tables like table 6 are not presented because they are bulky.

Table 6. Calculated energies and intermediate coupling coefficients of Helium $1s7i$ configuration in the magnetic field

H=0					
E, cm ⁻¹	3I_6	3I_7	3I_5	1I_6	g
196071.428891148	0.823432	0	0	-0.567416	1.01618125
196071.429352355	0	1.0000	0	0	1.14318857
196071.429772608	0	0	1.0000	0	0.832946667
196071.430106489	0.567416	0	0	0.823432	1.00768351
M = +1					
E, cm ⁻¹	3I_6	3I_7	3I_5	1I_6	
196071.428893514	0.823417	0.0028069	0.00158219	-0.567430	
196071.429355026	-0.00163931	0.9999954	-6.687 · 10 ⁻⁶	0.00256787	
196071.429774552	0.000327751	-1.157 · 10 ⁻⁶	0.999995	0.00326396	
196071.430108845	0.567434	-0.00118424	-0.00287358	0.823413	
M = 0					
E, cm ⁻¹	3I_6	3I_7	3I_5	1I_6	
196071.428891142	0.823429	0.00283789	0.00160386	-0.567410	
196071.429352358	-0.00165819	0.9999953	-6.678 · 10 ⁻⁶	0.00259506	
196071.429772607	0.000334914	-1.363 · 10 ⁻⁶	0.999994	0.00331263	
196071.430106493	0.567417	-0.00119598	-0.00291776	0.823425	
M = -1					
E, cm ⁻¹	3I_6	3I_7	3I_5	1I_6	
196071.428888770	0.823441	0.0028106	0.0015807	-0.567392	
196071.429349689	-0.00164307	0.9999954	-6.623 · 10 ⁻⁶	0.00256902	
196071.429770663	0.000332712	-1.227 · 10 ⁻⁶	0.999995	0.00326866	
196071.430104141	0.567399	-0.00118318	-0.00288033	0.823437	

In the Table 7 results of calculations of gyromagnetic ratios (formula (5) and coupling coefficients in the Table 6) from Zeeman splitting are presented. The range of linearity of magnetic field of all considered configurations is indicated. The coefficients of intermediate coupling of $1s7i$ and $1s8i$ configurations are determined when $H = 0.05$ Oe, $1s9i$ and $1s10i$ configuration when $H = 0.03$ Oe.

Table 7. The gyromagnetic ratios of $1sni$ configurations levels, determined from Zeeman splitting in the linear range of the magnetic field

	g-factors			
	1s7i	1s8i	1s9i	1s10i
3I_6	1.016181(1.4)	1.016182(1.3)	1.016182(0.7)	1.016183(1.0)
3I_7	1.143187(0.3)	1.143186(0.3)	1.143186(0.5)	1.143185(0.4)
3I_5	0.832948(0.5)	0.832950(0.8)	0.832950(0.4)	0.832952(0.3)
1I_6	1.007682(0.8)	1.007681(0.7)	1.007681(1.5)	1.007680(1.1)

Note: In the brackets is indicated the maximal error in the last value of digits of the values of $M = +1, 0, -1$

The range of linearity (in Oe)

	1s7i	1s8i	1s9i	1s10i
3I_6	0 – 0.09	0 – 0.07	0 – 0.06	0 – 0.05
3I_7	0 – 0.14	0 – 0.12	0 – 0.1	0 – 0.08
3I_5	0 – 0.27	0 – 0.22	0 – 0.18	0 – 0.16
1I_6	0 – 0.1	0 – 0.08	0 – 0.07	0 – 0.06

Comparing the gyromagnetic ratios from the Table 7 (in the magnetic field) with similar values in the Table 3 (in the absence of the field). It is seen that, the error is in order of

10^{-5} , which is the same for 3I_6 and 1I_6 levels. For the 3I_7 level, the g-factors determined from the Zeeman splitting is a little lower, and the 3I_5 level is a little higher as compared to similar LS-couplings (we remind that, $g^{LS}(^3I_7) = 1.1431886$; $g^{LS}(^3I_5) = 0.8329467$ see part of the Table 1 below). Thus, the levels with $J = 7$ and $J = 5$ also show a non-significant digression from the LS-coupling.

Let's go to particularities of the Zeeman splitting – the crossing and the anticrossing of magnetic components. Fig.2 shows a general view of level splitting for example in the $1s7i$ configuration in the magnetic field 0 - 12 Oe. In the Helium $1sni$ configurations, the crossings of magnetic components with $\Delta M = \pm 1, \pm 2$ are many and they start with small values of the field strength. In the present paper we are not going to dwell on this kind of crossing due to the absence of the experimental data with which we can compare the results of our calculations. Part of the crossing in Fig 2 is denoted by cycles with the labels of the crossing components and the corresponding values of the magnetic field H.

The most interesting are the anticrossing components, there are about three in the considered configuration. Furthermore in the experimental domain, the anticrossings are easy to determine, as there is no special exigency on increasing the population of the levels.

On Fig.3 the anticrossing of magnetic components in increasing order are presented, on Fig.4 the fragment of the most narrow crossing is shown also in increasing order. In the Table 8 the minimal energy intervals in the waists of anticrossing and their corresponding values of the magnetic fields for all the four considered $1sni$ configurations are represented.

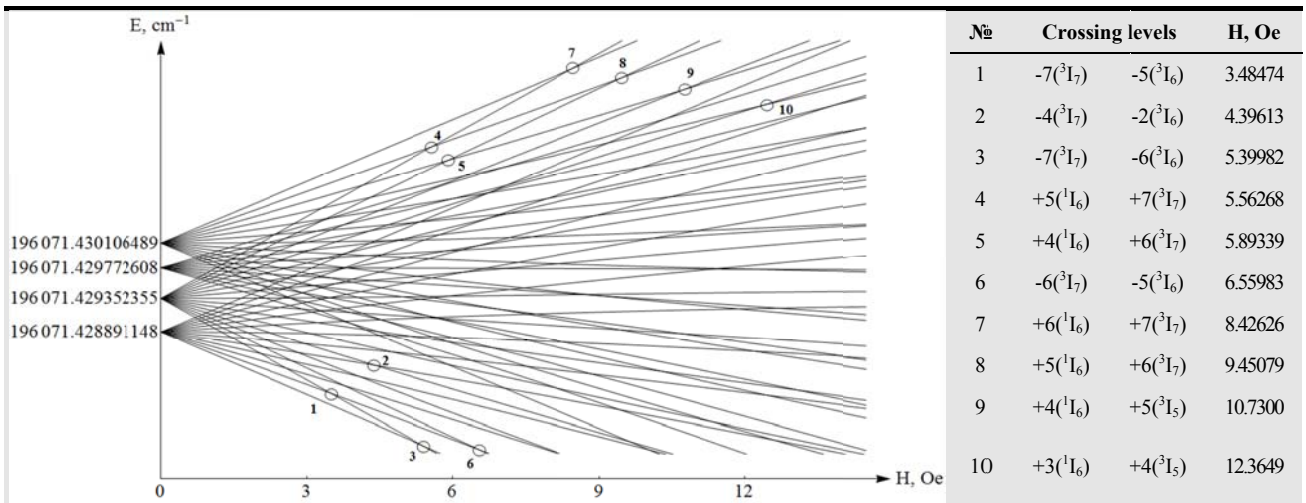


Fig.2. General View of the Zeeman splitting levels of the Helium atom in $1s7i$ configuration

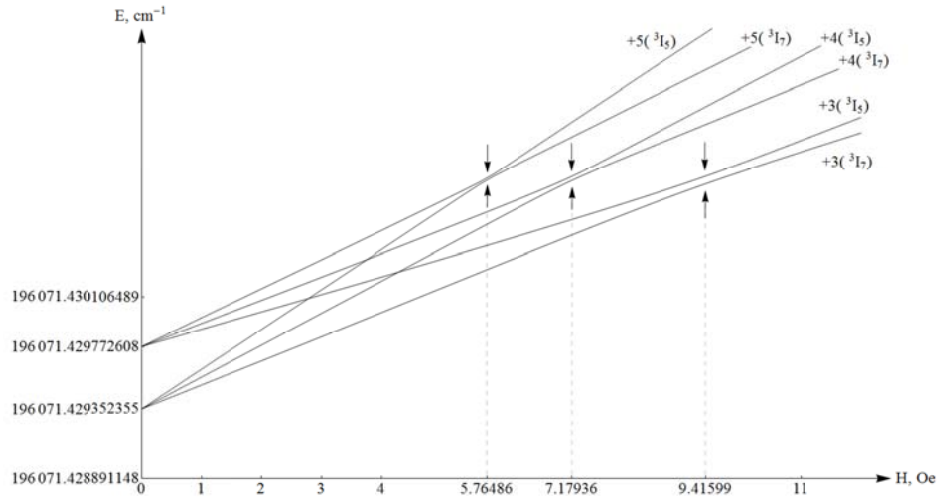


Fig.3. Dependence of energies of Zeeman components with $\Delta M = 0$ in the magnetic field (the anticrossings are denoted by arrows)

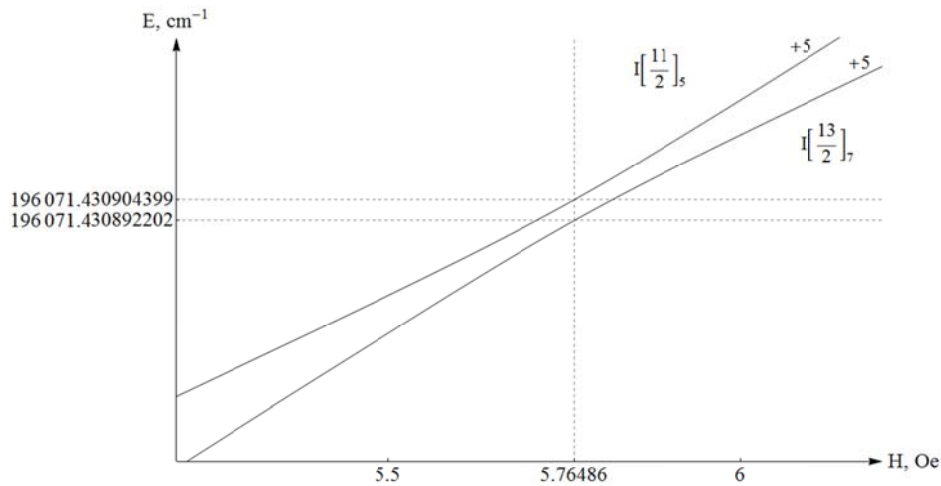


Fig.4. Fragment of the anticrossing of the magnetic components $+5(³I₅) - +5(³I₇)$ (on the figure the levels are written in the LK-coupling approximation)

Table 8. Minimal energy intervals in the anticrossing waists with $\Delta M = 0$ and their corresponding magnetic field values

Crossing sublevels		1s7i		1s8i		1s9i		1s10i	
Upper	Lower	$\Delta E, \text{cm}^{-1}$	H, Oe						
$+5(³I₅)$	$+5(³I₇)$	0.000012197	5.76486	$8.17077 \cdot 10^{-6}$	3.86199	$5.73472 \cdot 10^{-6}$	2.71153	$4.18315 \cdot 10^{-6}$	1.97733
$+4(³I₅)$	$+4(³I₇)$	0.0000273514	7.17936	0.0000183227	4.80959	0.0000128607	3.37686	$9.38062 \cdot 10^{-6}$	2.46249
$+3(³I₅)$	$+3(³I₇)$	0.0000514992	9.41599	0.0000344994	6.30796	0.0000242176	4.42891	0.0000176626	3.22966

It's known that, the anticrossing sublevels are from different terms. If the considered systems were near the LS-coupling, the components of the $³I$ and $¹I$ terms must be anticrossing. From Fig. 2-4 and the Table 8 it's seen that all the anticrossing $1sni$ configuration are coming from $³I₇$ and $³I₅$ levels (written in the LS-coupling approximation). Earlier it was shown in paragraph 1 (Fig.1) and in paragraph 4 (the Table 3) that, the $1sni$ configurations were far from LS-coupling and occupied an intermediate position between LS and LK-type vector couplings near the LK-coupling. In the LK-coupling approximation the $³I₇$ and $³I₅$ levels are written respectively as:

$$I \left[\frac{13}{2} \right]_7 \text{ and } I \left[\frac{11}{2} \right]_5 \tag{16}$$

They are different terms, because they have different values of the intermediate momentum K (in square brackets (16)), as was expected.

Let us summarize the results of this work. The high excited $1sni$ Helium atom configurations (the fine structure) have been theoretically investigated both in the magnetic field (based on the Zeeman splitting) so without (the fine structure). In both cases during the numerical diagonalization of the corresponding energy operator matrixes, the coefficients of the intermediate coupling and the gyromagnetic ratios, which do not exist in the majority

of Helium atom configurations in the experimental domain, were obtained.

References

- [1] NIST Atomic Spectra Database Levels Data, 2009.
- [2] NIST ASD Levels Output, 2013.
- [3] A.P.Yutsis, and A.Yu.Savukinas, Mathematical Foundations of the Atomic Theory, Vil'nyus, 1973 [in Russian].
- [4] D.A.Varshalovich, A.N.Moskalev, and V.K.Khersonskii, Quantum Theory of the Angular Momentum, Leningrad, 1975.
- [5] I.I.Sobelman, Introduction to the Theory of Atomic Specters, Moscow, 1963 [in Russian].
- [6] J.B.Green, and J.F.Eichelberger, Phys.Rev., 56 (1), 51, 1939.
- [7] G.P.Anisimova, O.A.Dolmatova, A.P.Gorbenko, and M.Choffo, American Journal of Modern Physics, 2 (6), 334, 2013.
- [8] V.Kaufman, and J.Sugar, J. Phys. Chem. Rev. Data, 17 (4), 1679, 1988.